

Metabolomics-based discovery of a metabolite that enhances oligodendrocyte maturation

Brittney A Beyer^{1,2,8}, Mingliang Fang^{3,7,8}, Benjamin Sadrian², J Rafael Montenegro-Burke³, Warren C Plaisted², Bernard P C Kok⁴, Enrique Saez⁴, Toru Kondo⁵, Gary Siuzdak^{3,6*} & Luke L Lairson^{1*}

Endogenous metabolites play essential roles in the regulation of cellular identity and activity. Here we have investigated the process of oligodendrocyte precursor cell (OPC) differentiation, a process that becomes limiting during progressive stages of demyelinating diseases, including multiple sclerosis, using mass-spectrometry-based metabolomics. Levels of taurine, an aminosulfonic acid possessing pleotropic biological activities and broad tissue distribution properties, were found to be significantly elevated (~20-fold) during the course of oligodendrocyte differentiation and maturation. When added exogenously at physiologically relevant concentrations, taurine was found to dramatically enhance the processes of drug-induced *in vitro* OPC differentiation and maturation. Mechanism of action studies suggest that the oligodendrocyte-differentiation-enhancing activities of taurine are driven primarily by its ability to directly increase available serine pools, which serve as the initial building block required for the synthesis of the glycosphingolipid components of myelin that define the functional oligodendrocyte cell state.

Multiple sclerosis is a debilitating autoimmune disease characterized by primary demyelination of axons and subsequent neuronal dysfunction^{1,2}. Disease remission in multiple sclerosis is dependent on a regenerative process known as remyelination, which persists throughout adulthood and involves the migration and subsequent differentiation of OPCs, leading to the formation of newly formed oligodendrocytes²⁻⁷. OPCs are found to be abundantly present in chronic lesions of multiple sclerosis patients, and as such, local inhibition of OPC differentiation is thought to be causative in multiple sclerosis disease progression^{8,9}. A promising complementary approach to the treatment of multiple sclerosis, as well as other demyelinating diseases, therefore, involves the identification of pharmacological agents that directly stimulate the process of remyelination by enhancing the process of OPC differentiation^{2,10-13}. Recently, our lab and others have identified multiple drug candidates using high-throughput screening approaches that induce OPC differentiation *in vitro* and enhance remyelination *in vivo* in relevant rodent models¹⁴⁻¹⁸. However, additional potential treatment strategies, as well as a systems biology level of understanding of the mechanisms associated with OPC differentiation and function, are clearly still needed.

Metabolomic profiling can not only define cell state and function, but also can play a critical role in understanding processes associated with cellular differentiation and reprogramming¹⁹⁻²⁴. Several recent studies have demonstrated the important role of small-molecule metabolites in mediating cellular reprogramming and differentiation. For example, the production of glycolytic end products is found to be elevated in induced pluripotent stem cells (iPSCs) following reprogramming, and somatic cell oxidative bio-energetic transitions have been shown to facilitate nuclear reprogramming²⁰. Similarly, using a global metabolomics approach, we have previously found that cell-type-dependent metabolite oxidation plays a key role in regulating embryonic stem cell (ESC) differentiation¹⁹. In

a very recent study, naive ESCs were found to maintain a high level of intracellular α -ketoglutarate, which is an important cofactor for demethylation reactions that help maintain the pluripotent state²³. Compared to metabolomics-based studies of iPSCs and ESCs, the role of cellular metabolism, and notably central carbon metabolism, in the regulation of OPC differentiation and myelination remains poorly understood. Herein, with the goal of identifying mechanisms and molecules that could be used in the development of new treatment strategies for multiple sclerosis, we have used a global metabolomics approach to successfully identify endogenous metabolites that are significantly altered over the course of the OPC differentiation process and can serve to directly impact cell fate.

RESULTS

Global comparative metabolomic analysis

Differentially regulated metabolites from OPCs and mature oligodendrocyte (OL) cells were characterized by MS-based untargeted metabolomic and lipidomic analysis, involving hydrophilic interaction chromatography (HILIC) and reversed-phase liquid chromatography (RP), respectively, combined with electrospray ionization quadrupole time-of-flight mass spectrometry (LC-ESI-QTOF-MS) (Supplementary Results, Supplementary Fig. 1). Using established conditions for the *in vitro* differentiation of purified primary OPC cultures generated by immunopanning of rat optic nerves¹⁷, we differentiated cells over the course of 6 d to a mature myelin basic protein positive (MBP⁺) fate using triiodothyronine (T3), a known inducer of OPC differentiation²⁵. We performed metabolomics analysis on normalized lysates derived from OPCs cultured for 6 d in basal media (2 ng/mL PDGF $\alpha\alpha$) containing T3 or DMSO vehicle. Western-blot-based analysis of MBP in lysates derived from parallel cultures was used to confirm relative differentiation efficiency. Consistent with previous studies of ESC cultures¹⁹, RP lipidomics showed more altered lipids with a highly unsaturated

¹Department of Chemistry, The Scripps Research Institute, La Jolla, California, USA. ²The California Institute for Biomedical Research, La Jolla, California, USA. ³Center for Metabolomics and Mass Spectrometry, The Scripps Research Institute, La Jolla, California, USA. ⁴Department of Molecular Medicine, The Scripps Research Institute, La Jolla, California, USA. ⁵Division of Stem Cell Biology, Institute for Genetic Medicine, Hokkaido University, Sapporo, Japan. ⁶Department of Molecular and Computational Biology, The Scripps Research Institute, La Jolla, California, USA. ⁷Present address: School of Civil and Environmental Engineering, Nanyang Technological University, Singapore, Singapore. ⁸These authors contributed equally to this work. *e-mail: llairson@scripps.edu or siuzdak@scripps.edu

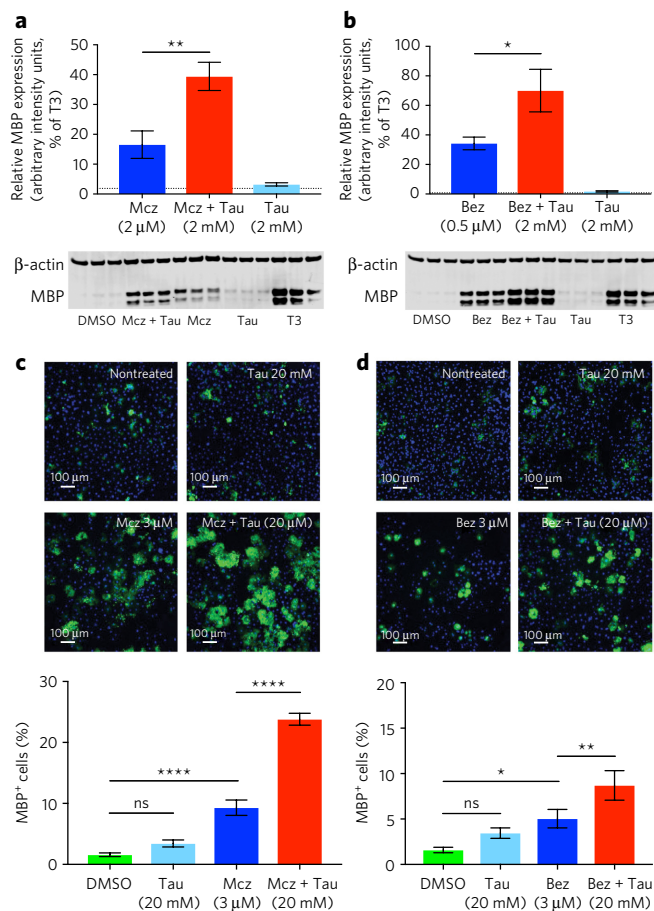


Figure 2 | Impact of taurine treatment on the efficacy of drug-induced OPC differentiation. (a) MBP expression following 6 d of differentiation with miconazole (Mcz, 2 μ M), miconazole (2 μ M) plus taurine (Tau, 2 mM) or taurine (2 mM) alone. Miconazole treatment initiated at day 0, and taurine treatment initiated at day 2. The data are mean \pm s.d. ($n = 3$ replicate cell cultures) and normalized to MBP levels observed following induction with T3 (1 μ M). Dotted line represents DMSO activity. β -actin was used as internal control. Full gel provided in **Supplementary Figure 4a**. (b) MBP expression following 6 d of differentiation with benzotropine (Bez; 0.5 μ M), benzotropine (0.5 μ M) plus taurine (2 mM) or taurine (2 mM) alone. Benzotropine treatment initiated at day 0, and taurine treatment initiated at day 2. The data are mean \pm s.d. ($n = 3$ replicate cell cultures) and are normalized to MBP levels observed following induction with T3 (1 μ M). Dotted line represents DMSO activity. β -actin was used as an internal control. Full gel provided in **Supplementary Figure 4b**. (c,d) Automated immunofluorescence analysis (MBP, green; DAPI, blue) of DMSO, taurine (20 mM), miconazole (3 μ M), miconazole (3 μ M) plus taurine (20 mM), benzotropine (3 μ M), and benzotropine (3 μ M) plus taurine (20 mM). Drug and taurine treatment initiated at day 0. Data are mean \pm s.d. for the percentage of MBP-positive cells per well ($n = 4$ replicate cell cultures). ns, no significance; * $P < 0.05$; ** $P < 0.01$; **** $P < 0.0001$. Scale bars, 100 μ m.

Following 14 d of neuron–OPC co-culture, 2 mM taurine was found to significantly increase the observed index of MBP colocalization with axons in cultures treated with either benzotropine or miconazole to induce OPC differentiation (**Fig. 3a–c**).

Differentiation-state-dependent effects of taurine

During the course of *in vitro* and *in vivo* OPC differentiation, cells transition through an immature MBP⁻ ‘premyelinating’ oligodendrocyte state^{2,28}. In our assay system, this occurs between day 2 and 3 of differentiation¹⁷. To determine the stage of OPC differentiation

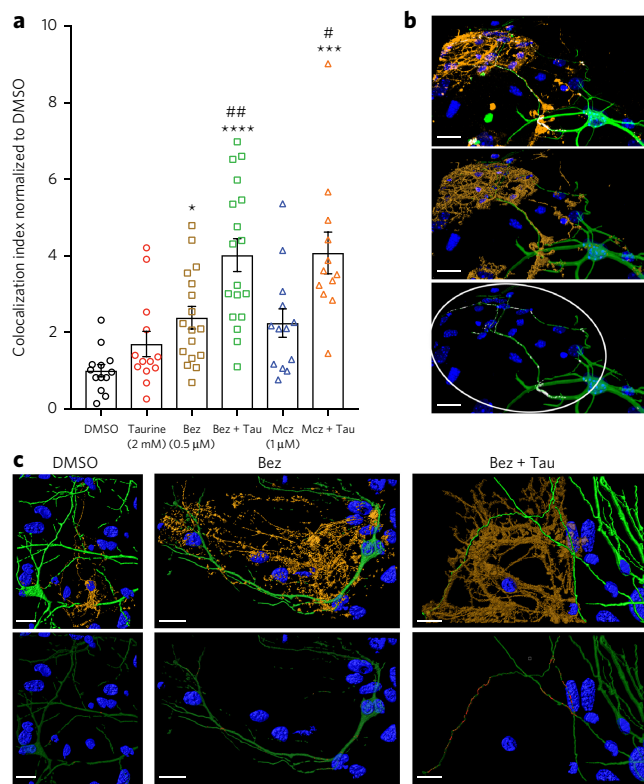


Figure 3 | Impact of taurine treatment on observed indices of MBP colocalization with co-cultured axons. (a) Quantification of MBP colocalization with the axons of primary mouse cortical neurons co-cultured with OPCs following 14 d of treatment. Cultures were treated with 0.5 μ M benzotropine (Bez) or 1 μ M miconazole (Mcz) in the presence or absence of 2 mM taurine. The data are mean \pm s.e.m.; * = significance of treatments vs. DMSO; # = significance of co-treatment vs. drug alone; one symbol: $P < 0.05$, two symbols: $P < 0.01$, four symbols: $P < 0.0001$; $n = 13$ technical replicates for DMSO, Tau, Mcz, Mcz + Tau; $n = 17$ technical replicates for Bez; $n = 19$ technical replicates for Bez + Tau. (b) Representative confocal microscopy fluorescence imaging of a co-culture following 14 d of treatment (DAPI, blue; TuJ1, green; MBP, orange). White indicates regions of colocalization (scale bars, 20 μ m). Middle, 3D rendering of the image above used to quantify colocalization index (as shown on the bottom with the MBP channel removed to reveal sites of colocalization of TuJ1 and MBP). The colocalization index (see methods) is quantified on neuronal processes contained within the oligodendrocyte region of interest (ROI, circled) and normalized using DMSO control. (c) Example of rendered fluorescent confocal images of differentiated OPCs co-cultured with cortical neurons (labeled as above). The bottom copy of each pair illuminates the areas of colocalization overlap in between the two cell types in red to demonstrate proportions of MBP⁺ neuronal processes.

at which taurine enhances drug efficacy, we tested the effect of taurine at various time points by initiating dosing with taurine at days 0 to 5 and evaluating cell cultures at day 6. The most significant impact on MBP expression was observed when taurine was added between days 1 and 3, with addition on day 0 being significantly less efficacious (**Supplementary Fig. 5a,b**), suggesting that taurine facilitates the maturation of premyelinating OLGs rather than inducing cell cycle exit and/or the differentiation of fully immature proliferating OPCs. Consistently, addition of taurine to basal (DMSO vehicle) or drug-induced differentiation conditions on day 0, 1 or 3 was found to have a minimal, albeit statistically significant, impact on the number of residual immature A2B5⁺ OPCs at day 3 or 6 (**Supplementary Fig. 5c,d**). This temporal trend also coincided

with the decrease of the oxidative stress marker GSH/GSSG at day 3 (Supplementary Fig. 3).

Impact of taurine on mitochondrial function

In addition to its ability to function in the maintenance of buffer capacity, redox potential, osmoregulation and membrane stabilization, taurine can modulate ion flux and act as a neuromodulator to control synaptic transmission and enhance or preserve mitochondrial function in response to increased secondary metabolite demand or excitotoxicity^{29,30}. Specifically, taurine has been shown to be able to regulate intracellular calcium levels and preserve mitochondrial energy metabolism in glutamate-challenged cultures of cerebellar granule cells³¹. When proliferating OPCs differentiate to OLs that function to produce myelin, mitochondrial energy requirements are presumably challenged in response to the activation of phospholipid biosynthetic pathways. We therefore examined oxygen consumption rates (OCR) associated with mitochondrial respiratory activity using an XFe96 Seahorse instrument. Addition of 2 mM taurine to culture media significantly increased OCR values at day 6 under basal, as well as bupropion- or miconazole-induced, differentiation conditions (Fig. 4a). Interestingly, miconazole treatment alone was found to have a negative impact on OCR values compared to DMSO or bupropion treatment (Fig. 4a). These observations are in agreement with the ability of taurine to enhance mitochondrial function in both OPCs and OLs. Consistent with the critical dependence of OPCs and OLs on mitochondrial function, treatment with the mitochondrial function inhibitors oligomycin or rotenone induced cell death within 24 h at all concentrations tested, which precluded the ability to evaluate the impact of taurine rescue following treatment with these agents in the differentiation assay.

Impact of taurine on OPC and OL survival

Related to a beneficial impact on the process of mitochondrial function, the observed overall differentiation-enhancing effect of taurine could be derived from a protective effect associated with inhibition of apoptosis. Substantial apoptosis would be expected to occur as OPCs exit the cell cycle in response to growth-factor withdrawal, as well as during the process of pre-oligodendrocyte maturation. As such, we evaluated the impact of taurine addition on cell survival and apoptosis over the course of the oligodendrocyte differentiation process using CellTiter Glo and Caspase-Glo 3/7 assays. When added at day 0 (Supplementary Fig. 6a,c) or day 3 (Fig. 4b; Supplementary Fig. 6b,d), taurine was found to decrease caspase-3/7 activation 24 h following supplementation under drug-induced differentiation conditions (i.e., 1 μ M T3, 0.5 μ M bupropion or 2 μ M miconazole). This finding is consistent with the observed beneficial impact on overall survival at day 6, as described above (Supplementary Fig. 4c,d). Taurine was also found to significantly inhibit apoptosis in OPCs treated with staurosporine, which served as a positive control for apoptosis induction (Supplementary Fig. 6a,b). Taurine did not display any impact on apoptosis or survival under basal (DMSO vehicle) differentiation conditions (Fig. 4b; Supplementary Fig. 6a,b).

Impact of taurine on oxidative stress in OPCs and OLs

Oxidative stress has been demonstrated to disrupt oligodendrocyte differentiation by directly decreasing the expression of key pro-differentiation genes and increasing the expression of genes known to inhibit differentiation³². Furthermore, changes in intracellular redox state have been reported to be sufficient to drive the balance between self-renewal and differentiation during the course of OL differentiation³³. We evaluated the potential impact of taurine-mediated redox state modulation on OL differentiation efficiency by evaluating the impact of alternative reducing agents on basal (DMSO vehicle) or drug-induced OL differentiation. Although reduced glutathione (10 μ M GSH; Fig. 4c) had no significant effect on differentiation

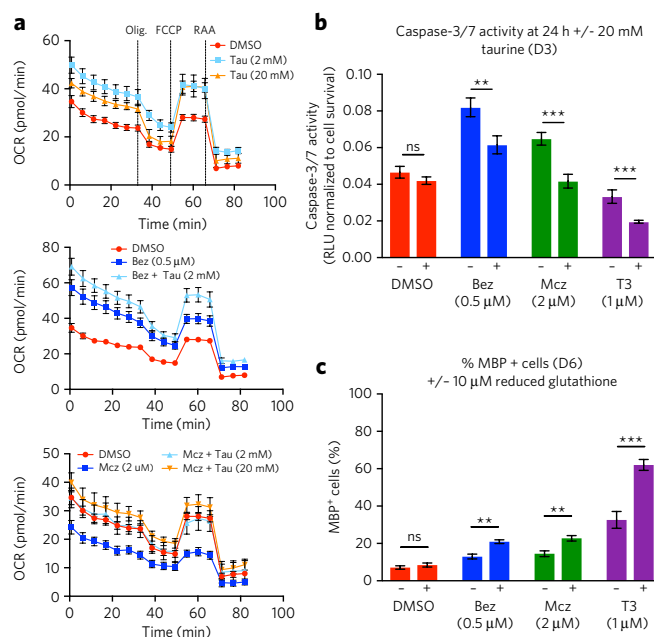


Figure 4 | The impact of taurine treatment on OL mitochondrial function and the role of redox state on OPC differentiation.

(a) Oxygen consumption rate (OCR; pmol/min) of OPCs (40,000 cells/well) treated for 6 d with taurine (Tau; 2 or 20 mM) and DMSO, bupropion (Bez; 0.5 μ M) with and without 2 mM taurine or miconazole (Mcz; 2 μ M) with and without 2 and 20 mM taurine. Complex activity was measured at baseline, as well as after the successive addition of 1 μ M oligomycin (Olig.), 2 μ M carbonyl cyanide 4-(trifluoromethoxy) phenylhydrazone (FCCP) and 2 μ M rotenone and antimycin A (RAA). The data are mean \pm s.d. ($n = 12$ technical replicates). The dashed line in the top panel indicates the addition of the compound indicated. (b) Quantification of caspase-3/7 activation 24 h post-aurine addition on day 3 (D3), after treatment with DMSO, miconazole (2 μ M), bupropion (0.5 μ M), or T3 (1 μ M) on day 0. Data are mean \pm s.d. of the luminescence (RLU) normalized to corresponding cell survival per well ($n = 3$ replicate cell cultures). (c) Quantification of MBP-positive OLs based on MBP immunofluorescent analysis on day 6 (D6) post-treatment with DMSO, miconazole (2 μ M), bupropion (0.5 μ M), or T3 (1 μ M), following co-treatment with or without reduced glutathione (10 μ M). Data are mean \pm s.d. for the percentage of MBP-positive cells per well ($n = 3$ replicate cell cultures). ns, no significance; ** $P < 0.01$; *** $P < 0.001$.

efficiency under basal conditions (DMSO), it was found to significantly enhance the overall efficiency of T3-induced differentiation (Fig. 4c; Supplementary Fig. 7a), as well as the observed total nuclei count (Supplementary Fig. 7b). Reduced glutathione was also found to enhance the overall efficiency of bupropion- or miconazole-induced differentiation, albeit to a lesser extent than what is observed following taurine addition (Fig. 4c; Supplementary Fig. 7a), and the impact on total cell number was not found to be significant (Supplementary Fig. 7b). As such, modulation of redox state could be a beneficial contributing mechanism that serves to enhance the process of drug-induced OL differentiation. However, the inability to fully recapitulate the activity of taurine with alternative biological reducing agents indicates that this activity is not likely the sole mechanism by which taurine enhances the process of OL differentiation.

Taurine-induced metabolomic changes

To identify metabolic changes that are directly impacted by exogenous taurine supplementation in OPCs and OLs, binary global metabolomics analysis was performed between cell lysates following

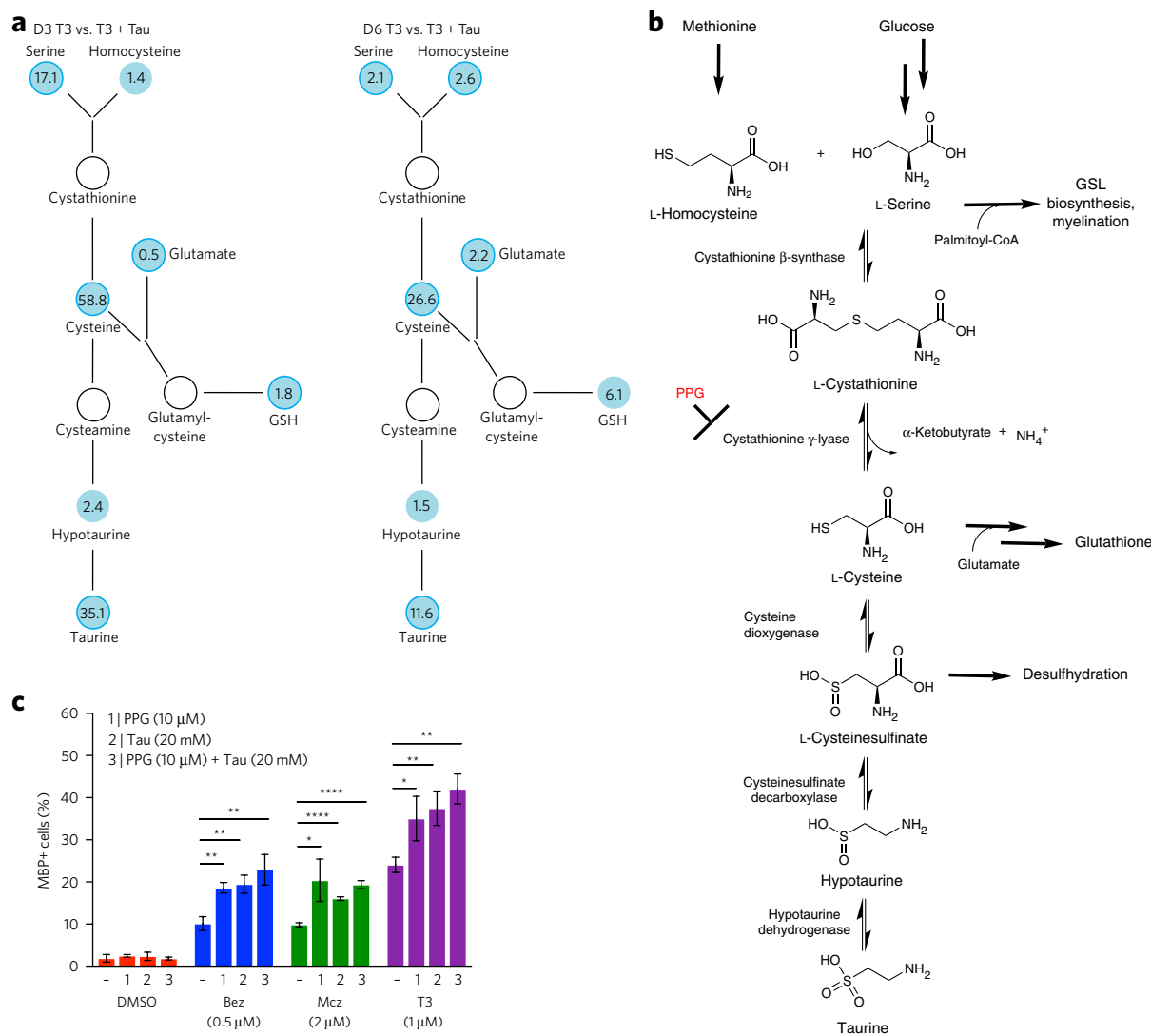


Figure 5 | Binary global metabolomics analysis of taurine co-treatment and evaluation of the impact of inhibition of taurine biosynthesis on OL differentiation. (a) Binary global metabolomics analysis of the impact of taurine (Tau, 20 mM) supplementation on pre-myelinating OLs (day 3, D3) and OLs (day 6, D6) differentiated using T3 (1 μM). Numbers represent fold changes of metabolites, with values smaller than one suggesting downregulation and values larger than one suggesting upregulation. White indicates nondetected (i.e., below the limit of detection). Darker circles represent $P < 0.05$. (b) Taurine biosynthesis pathway highlighting the relationship to glycosphingolipid (GSL) biosynthesis and the impact of propargylglycine (PPG)-mediated inhibition of cystathionine γ -lyase on taurine and GSH production. (c) Quantification of MBP-positive OLs based on MBP immunofluorescence analysis on day 6 post-treatment with DMSO, miconazole (2 μM), benzotropine (0.5 μM), or T3 (1 μM), following addition of PPG (10 μM), taurine (20 mM) or PPG (10 μM) and taurine (20 mM). Data are mean \pm s.d. for the percentage of MBP-positive cells per well ($n = 3$ replicate cell cultures). ns, no significance; * $P < 0.05$; ** $P < 0.01$; **** $P < 0.0001$.

treatment with a given differentiation-inducing agent (i.e., T3, benzotropine or miconazole) in the presence or absence of 20 mM taurine for 3 or 6 d. This pair-wise analysis allowed drug-specific and differentiation-state-dependent effects to be filtered out, thereby enabling the identification of metabolomic changes that are specific to taurine supplementation. This analysis revealed that relatively few metabolite pools are impacted by taurine supplementation. However, we observed significantly increased serine and cysteine pools in lysates derived from taurine-treated OPCs following 3 d of drug-induced differentiation using T3 (1 μM, 17.1- and 58.8-fold, respectively; **Fig. 5a**), benzotropine (0.5 μM, 10.0- and 154.4-fold, respectively; **Supplementary Fig. 8a**) or miconazole (2 μM, 19.4- and 76.5-fold, respectively; **Supplementary Fig. 8b**). Similarly, at day 6, we observed that serine and cysteine levels were significantly higher in lysates derived from taurine-treated OPCs differentiated using T3 (1 μM, 2.1- and 26.6-fold, respectively; **Fig. 5a**), benzotropine

(0.5 μM, 13.4- and 44.7-fold, respectively; **Supplementary Fig. 8a**) or miconazole (2 μM, 92.5- and 47.2-fold, respectively; **Supplementary Fig. 8b**). We found slightly higher GSH levels in lysates derived from taurine-treated OPCs differentiated using T3 (1 μM) at day 3 (1.8-fold; **Fig. 5a**) and day 6 (6.1-fold; **Fig. 5a**). Changes in GSH and glutamate were found to be only minimally altered in benzotropine- (0.5 μM) or miconazole (2 μM)-treated cultures at both time points (**Supplementary Fig. 8a,b**). Collectively, the observed impacts on metabolite pools at different stages of the differentiation process imply that the addition of taurine reduces the need for serine and cysteine biosynthesis and/or increases available pools of these metabolites for alternative biosynthetic functions that are potentially required for OL maturation and/or function. Indeed, under optimal conditions of T3-induced differentiation, lower observed serine levels at day 6 following taurine supplementation as compared to those observed at day 3 (**Fig. 5a**) suggests that

serine pools derived from taurine are consumed by other biosynthetic pathways in mature OLs.

Direct effect of taurine on OPC differentiation

An alternative mechanism by which exogenously added taurine could enhance the process of drug-induced differentiation is by directly modulating the activity of a receptor or ion transporter (as described above), which serves to either stimulate or inhibit OL differentiation. Indeed, M1/M3 muscarinic receptor antagonism, and the associated altered intracellular calcium levels, is an essential component of the mechanism of bntropine- and clemastine-induced OPC differentiation^{17,18}. To determine whether taurine itself contributes to the process of OPC differentiation, as opposed to having indirect effects on redox state or mitochondrial health and cell viability, we inhibited endogenous taurine biosynthesis using propargylglycine (PPG). PPG is an irreversible inhibitor of cystathionine γ -lyase, which can be used to inhibit the conversion of L-cystathionine to L-cysteine and downstream taurine biosynthesis in cells³⁴. Importantly, this also results in the inhibition of glutathione biosynthesis (Fig. 5b). The relative contribution of these two potential mechanisms could therefore be elucidated by adding either exogenous taurine or glutathione in combination with PPG. If taurine acts by a mechanism involving direct modulation of the function of an essential protein, PPG treatment would inhibit oligodendrocyte differentiation, and this effect could be rescued by exogenously adding back taurine. Similarly, if the OPC differentiation-enhancing activity of taurine is derived exclusively from a redox effect that results from the combined activities of increased levels taurine and glutathione, PPG treatment would inhibit oligodendrocyte differentiation, and this effect could be rescued by exogenously adding back reduced glutathione and/or other alternative biological reducing agents. However, paradoxically, PPG (10 μ M) was found to significantly enhance the observed efficacy of all drug-induced differentiation conditions when added at day 0 (Fig. 5c; Supplementary Fig. 9a). Furthermore, the magnitude of this effect was found to be similar to the effect of adding taurine itself to any given drug-induced differentiation condition, including T3 (Fig. 5c). Consistent with the effect of taurine addition, PPG had virtually no impact on differentiation efficiency under basal vehicle-treated conditions. (Fig. 5c). Importantly, PPG was not found to impact overall survival in OPC cultures treated with DMSO, bntropine (0.5 μ M) or miconazole (2 μ M) (Supplementary Fig. 9b). In the case of T3 (1 μ M) treatment, PPG (10 μ M) was actually found to enhance overall cell number (Supplementary Fig. 9b). These observations make it unlikely that taurine itself stimulates a pro-differentiation process by directly interacting with a relevant receptor or alternative protein target, but rather that exogenous taurine enhances OL differentiation by serving as a feedstock to produce a limiting metabolite pool. Furthermore, as PPG negatively impacts GSH biosynthesis, and, as GSH and glutamate levels were found to be only minimally impacted by taurine supplementation (Fig. 5a; Supplementary Fig. 8a,b), it is unlikely that a redox state effect is the primary mechanism contributing to the overall beneficial impact of taurine supplementation on OL differentiation and maturation.

DISCUSSION

This study used unbiased global metabolomics together with targeted analyses to identify altered metabolite pools associated with the process of OL differentiation and maturation. In addition to the significant observed changes that were anticipated in lipid metabolite profiles, many hydrophilic small-molecule metabolites were identified as being highly altered. Several of these metabolites were found to dramatically improve the processes of OPC differentiation when co-treated with various mechanistically unrelated remyelination-enhancing drugs. These findings provide support for the

notion that cell state and/or cell fate can be effectively modulated using strategies that involve supplementation with endogenously produced upregulated metabolites that are associated with the desired phenotype. Specifically, several exogenously supplemented metabolites that were found to increase significantly in mature OLs when compared to immature OPCs—most notably taurine—were found to significantly enhance the processes of OL differentiation.

Mechanistic studies suggest that although taurine supplementation can impact the processes of mitochondrial function and oxidative stress in a beneficial manner in this system, neither of these effects alone fully account for the observed differentiation- and maturation-enhancing activities of taurine. Surprisingly, the effect of taurine supplementation was found to be fully recapitulated when endogenous taurine biosynthesis, as well as GSH production, was blocked via the inhibition of an upstream enzyme. This seemingly paradoxical finding suggests that the primary mechanism by which exogenous taurine supplementation enhances OL differentiation is by reversing pathway flux. This notion is consistent with the results of binary global metabolomics analysis, which indicated that serine and cysteine are the most altered metabolite pools impacted by exogenous taurine addition. A reversal in flux, and/or taurine's ability to serve as an alternative feedstock, results in dramatically increased pools of serine, which serves as a primary building block for the glycosphingolipid (GSL) biosynthesis that is required to produce myelin.

GSL biosynthesis begins with the condensation of L-serine and palmitoyl-CoA to form 3-ketosphinganine and, subsequently, ceramide, which is the common precursor of sphingomyelin, gangliosides and galactolipids³⁵. Increased flux through the GSL biosynthetic pathway would impact OL maturation both by directly increasing the production of functional biomolecules that define the OL cell state and by modulating lipid signaling pathways that are known to impact differentiation at the transcriptional level. OL differentiation proceeds through a series of intermediate cell states that are not only defined by the presence of GSL surface antigens, but also directly impacted by the relative levels of specific GSLs³⁵. It has been demonstrated, for example, that GSL levels serve as sensors and transmitters of environmental information that can directly impact the expression of myelin genes and cause the arrest of terminal oligodendrocyte differentiation^{36,37}. Perhaps more importantly, enhanced flux through GSL biosynthetic pathways would lead to the direct production of myelin components and potentially the enhanced functional myelination of axons. When one considers that an essential function of an oligodendrocyte is the production of GSLs, which along with cholesterol make up the majority of the lipid components of myelin (~31% and ~27%, respectively³⁵), it is internally consistent that taurine supplementation can enhance OL maturation by directly enabling GSL biosynthesis.

The actual clinical relevance of our findings will require extensive preclinical evaluation involving quantitative analysis of the impact of taurine supplementation on *in vivo* drug-induced remyelination in the context of relevant rodent models of demyelinating disease. Nonetheless, the potential utility is appealing. Taurine is found in the brain at millimolar concentrations and it is a very well-tolerated agent that is actively transported across the blood-brain barrier³⁸. As such, taurine supplementation, in combination with existing standard of care drugs, could be a feasible treatment strategy to improve remyelination by enhancing GSL biosynthesis in OLs. A similar strategy involving oral formulation of high dose biotin, which serves as a cofactor for essential carboxylase enzymes required for fatty acid synthesis, has recently been demonstrated to provide benefit in patients with not-active progressive multiple sclerosis³⁹. Intriguingly, taurine has previously been identified as a dysregulated metabolite in animal models of multiple sclerosis disease, including nonhuman primate models⁴⁰, and its plasma levels can be used to distinguish PLP-induced experimental autoimmune

encephalomyelitis (EAE) mice from naive controls^{41–44}. At a minimum, these findings demonstrate the utility of global metabolomic analyses in the identification of endogenous metabolites that can serve to modulate cellular phenotypes.

Received 14 November 2016; accepted 11 October 2017;
published online 13 November 2017

METHODS

Methods, including statements of data availability and any associated accession codes and references, are available in the [online version of the paper](#).

References

- Pouly, S. & Antel, J.P. Multiple sclerosis and central nervous system demyelination. *J. Autoimmun.* **13**, 297–306 (1999).
- Franklin, R.J. & Ffrench-Constant, C. Remyelination in the CNS: from biology to therapy. *Nat. Rev. Neurosci.* **9**, 839–855 (2008).
- Gallo, V. & Armstrong, R.C. Myelin repair strategies: a cellular view. *Curr. Opin. Neurol.* **21**, 278–283 (2008).
- Dubois-Dalcq, M. *et al.* From fish to man: understanding endogenous remyelination in central nervous system demyelinating diseases. *Brain* **131**, 1686–1700 (2008).
- Franklin, R.J. & Hinks, G.L. Understanding CNS remyelination: clues from developmental and regeneration biology. *J. Neurosci. Res.* **58**, 207–213 (1999).
- Chamberlain, K.A., Nanesco, S.E., Psachoulia, K. & Huang, J.K. Oligodendrocyte regeneration: Its significance in myelin replacement and neuroprotection in multiple sclerosis. *Neuropharmacology* **110** Pt B, 633–643 (2016).
- Franklin, R.J.M. Why does remyelination fail in multiple sclerosis? *Nat. Rev. Neurosci.* **3**, 705–714 (2002).
- Wolswijk, G. Chronic stage multiple sclerosis lesions contain a relatively quiescent population of oligodendrocyte precursor cells. *J. Neurosci.* **18**, 601–609 (1998).
- Chang, A., Tourtellotte, W.W., Rudick, R. & Trapp, B.D. Premyelinating oligodendrocytes in chronic lesions of multiple sclerosis. *N. Engl. J. Med.* **346**, 165–173 (2002).
- Franklin, R.J. & Gallo, V. The translational biology of remyelination: past, present, and future. *Glia* **62**, 1905–1915 (2014).
- Huang, J.K. *et al.* Myelin regeneration in multiple sclerosis: targeting endogenous stem cells. *Neurotherapeutics* **8**, 650–658 (2011).
- Huang, J.K. *et al.* Retinoid X receptor gamma signaling accelerates CNS remyelination. *Nat. Neurosci.* **14**, 45–53 (2011).
- Lucchinetti, C.F., Noseworthy, J.H. & Rodriguez, M. Promotion of endogenous remyelination in multiple sclerosis. *Mult. Scler.* **3**, 71–75 (1997).
- Mei, F. *et al.* Identification of the kappa-opioid receptor as a therapeutic target for oligodendrocyte remyelination. *J. Neurosci.* **36**, 7925–7935 (2016).
- Najm, F.J. *et al.* Drug-based modulation of endogenous stem cells promotes functional remyelination *in vivo*. *Nature* **522**, 216–220 (2015).
- Buckley, C.E. *et al.* Drug reprofiling using zebrafish identifies novel compounds with potential pro-myelination effects. *Neuropharmacology* **59**, 149–159 (2010).
- Deshmukh, V.A. *et al.* A regenerative approach to the treatment of multiple sclerosis. *Nature* **502**, 327–332 (2013).
- Mei, F. *et al.* Micropillar arrays as a high-throughput screening platform for therapeutics in multiple sclerosis. *Nat. Med.* **20**, 954–960 (2014).
- Yanes, O. *et al.* Metabolic oxidation regulates embryonic stem cell differentiation. *Nat. Chem. Biol.* **6**, 411–417 (2010).
- Folmes, C.D.L. *et al.* Somatic oxidative bioenergetics transitions into pluripotency-dependent glycolysis to facilitate nuclear reprogramming. *Cell Metab.* **14**, 264–271 (2011).
- Shyh-Chang, N., Daley, G.Q. & Cantley, L.C. Stem cell metabolism in tissue development and aging. *Development* **140**, 2535–2547 (2013).
- Ito, K. & Suda, T. Metabolic requirements for the maintenance of self-renewing stem cells. *Nat. Rev. Mol. Cell Biol.* **15**, 243–256 (2014).
- TeSlaa, T. *et al.* α -Ketoglutarate accelerates the initial differentiation of primed human pluripotent stem cells. *Cell Metab.* **24**, 485–493 (2016).
- Huan, T. *et al.* Systems biology guided by XCMS Online metabolomics. *Nat. Methods* **14**, 461–462 (2017).
- Fernandez, M. *et al.* Thyroid hormone administration enhances remyelination in chronic demyelinating inflammatory disease. *Proc. Natl. Acad. Sci. USA* **101**, 16363–16368 (2004).
- Meissen, J.K. *et al.* Induced pluripotent stem cells show metabolomic differences to embryonic stem cells in polyunsaturated phosphatidylcholines and primary metabolism. *PLoS One* **7**, e46770 (2012).

- Panopoulos, A.D. *et al.* The metabolome of induced pluripotent stem cells reveals metabolic changes occurring in somatic cell reprogramming. *Cell Res.* **22**, 168–177 (2012).
- Fields, R.D. A new mechanism of nervous system plasticity: activity-dependent myelination. *Nat. Rev. Neurosci.* **16**, 756–767 (2015).
- Ramos-Mandujano, G., Hernández-Benítez, R. & Pasantes-Morales, H. Multiple mechanisms mediate the taurine-induced proliferation of neural stem/progenitor cells from the subventricular zone of the adult mouse. *Stem Cell Res.* **12**, 690–702 (2014).
- Shivraj, M.C. *et al.* Taurine induces proliferation of neural stem cells and synapse development in the developing mouse brain. *PLoS One* **7**, e42935 (2012).
- El Idrissi, A. & Trenkner, E. Growth factors and taurine protect against excitotoxicity by stabilizing calcium homeostasis and energy metabolism. *J. Neurosci.* **19**, 9459–9468 (1999).
- French, H.M., Reid, M., Mamontov, P., Simmons, R.A. & Grinspan, J.B. Oxidative stress disrupts oligodendrocyte maturation. *J. Neurosci. Res.* **87**, 3076–3087 (2009).
- Smith, J., Ladi, E., Mayer-Pröschel, M. & Noble, M. Redox state is a central modulator of the balance between self-renewal and differentiation in a dividing glial precursor cell. *Proc. Natl. Acad. Sci. USA* **97**, 10032–10037 (2000).
- Jurkowska, H., Stipanuk, M.H., Hirschberger, L.L. & Roman, H.B. Propargylglycine inhibits hypotaurine/taurine synthesis and elevates cystathionine and homocysteine concentrations in primary mouse hepatocytes. *Amino Acids* **47**, 1215–1223 (2015).
- Jackman, N., Ishii, A. & Bansal, R. Oligodendrocyte development and myelin biogenesis: parsing out the roles of glycosphingolipids. *Physiology (Bethesda)* **24**, 290–297 (2009).
- Bansal, R. & Pfeiffer, S.E. Reversible inhibition of oligodendrocyte progenitor differentiation by a monoclonal antibody against surface galactolipids. *Proc. Natl. Acad. Sci. USA* **86**, 6181–6185 (1989).
- Bansal, R. & Pfeiffer, S.E. Regulation of gene expression in mature oligodendrocytes by the specialized myelin-like membrane environment: antibody perturbation in culture with the monoclonal antibody R-mAb. *Glia* **12**, 173–179 (1994).
- Albrecht, J. & Schousboe, A. Taurine interaction with neurotransmitter receptors in the CNS: an update. *Neurochem. Res.* **30**, 1615–1621 (2005).
- Tourbah, A. *et al.* MD1003 (high-dose biotin) for the treatment of progressive multiple sclerosis: A randomised, double-blind, placebo-controlled study. *Mult. Scler.* **22**, 1719–1731 (2016).
- Hart, B.A. *et al.* ¹H-NMR spectroscopy combined with pattern recognition analysis reveals characteristic chemical patterns in urines of MS patients and non-human primates with MS-like disease. *J. Neurol. Sci.* **212**, 21–30 (2003).
- Gebregiworgis, T. *et al.* Potential of urinary metabolites for diagnosing multiple sclerosis. *ACS Chem. Biol.* **8**, 684–690 (2013).
- Mangalam, A. *et al.* Profile of circulatory metabolites in a relapsing-remitting animal model of multiple sclerosis using global metabolomics. *J. Clin. Cell. Immunol.* **4**, <http://dx.doi.org/10.4172/2155-9899.1000150> (2013).
- Preece, N.E. *et al.* Experimental encephalomyelitis modulates inositol and taurine in the spinal cord of Biozzi mice. *Magn. Reson. Med.* **32**, 692–697 (1994).
- Noga, M.J. *et al.* Metabolomics of cerebrospinal fluid reveals changes in the central nervous system metabolism in a rat model of multiple sclerosis. *Metabolomics* **8**, 253–263 (2012).

Acknowledgments

We gratefully acknowledge financial support from the National Institutes of Health (Grants R01 GM114368-02, R24 EY017540-04, P30 MH062261-10, P01 DA026146-02, and 1S10OD16357).

Author contributions

B.A.B., M.F., G.S. and L.L.L. initiated the project, developed the strategy and generated experimental design. B.A.B., W.C.P. and B.S. performed molecular biology and cell-based experiments. M.F. and J.R.M.-B. performed mass spectrometry and metabolomics experiments. B.P.C.K., B.A.B. and M.F. performed OCR experiments. B.A.B., M.F., W.C.P., B.S., J.R.M.-B., G.S. and L.L.L. interpreted data. E.S. and T.K. contributed essential ideas and comments. B.A.B., M.F., G.S. and L.L.L. wrote the manuscript.

Competing financial interests

The authors declare no competing financial interests.

Additional information

Any supplementary information, chemical compound information and source data are available in the [online version of the paper](#). Reprints and permissions information is available online at <http://www.nature.com/reprints/index.html>. Publisher's note: Springer Nature remains neutral with regard to jurisdictional claims in published maps and institutional affiliations. Correspondence and requests for materials should be addressed to L.L.L. or G.S.

ONLINE METHODS

Metabolites and small molecules. All the endogenous metabolites used in this study were from Sigma-Aldrich. Benztropine, miconazole and triiodothyronine (T3) were purchased from Sigma-Aldrich (Saint Louis, MO). All the chemicals used in this study have a purity $\geq 95\%$.

Rat primary optic nerve OPCs were isolated by panning ($>99\%$ A2B5⁺) and cultured in poly-D-lysine (10 $\mu\text{g}/\text{ml}$)-coated TC dishes in OPC culture media (Neurobasal Media, Invitrogen) supplemented with B27 without vitamin A (Invitrogen), 1 \times nonessential amino acids, 1 \times Glutamax, 1 \times anti-anti, β -mercaptoethanol and PDGF $\alpha\alpha$ (50 ng/ml ; Peprotech) at 37 °C with 5% CO₂. The culture medium was replaced every 48 h, and cells were collected before the confluency reached 60% to maintain a naive state. For differentiation, OPCs were plated at 1 million cells in one 10-cm Petri dish filled with differentiation media, which is identical to the culture media but with PDGF-AA at 2 ng/ml . T3 and DMSO were used as the positive control and negative control, respectively. Five replicates of cells were collected at different times (0, 3 and 6 d) for metabolomics studies.

Global metabolomics and lipidomics. Cells incubated in differentiation medium were collected at day 0, 3 and 6 for both the T3- and DMSO-treated OPCs. The cells were first rinsed with PBS twice to completely remove the culture medium and then scraped into a 1.5-mL Eppendorf vial using 500–1,000 μL PBS. Subsequently, cells were collected by aspirating the supernatant after centrifugation at 1,000 r.p.m. at 4 °C for 3 min. The global metabolites were extracted from cell pellets by a methanol:acetonitrile:water (2:2:1; v/v) solvent mixture. A volume of 600 μL cold solvent was added to each pellet, vortexed for 30 s, and soaked in liquid nitrogen for 1 min. Samples were then allowed to thaw at room temperature and then sonicated for 10 min. This freeze-thaw process was repeated twice. To further precipitate proteins, samples were incubated for 1 h at –20 °C and then centrifuged at 16,000g at 4 °C for 15 min. The protein concentration of the cells was measured in the final pellet after centrifugation using BCA assay. The resulting supernatant was removed and evaporated to dryness in a vacuum concentrator (Labconco CentriVap Benchtop). The dry extracts were then reconstituted in the appropriate volume of acetonitrile/water (1:1; v/v), normalized by the protein concentration with the lowest concentration approximately 50 μL , sonicated for 10 min, and centrifuged for 15 min at 16,000g and 4 °C to remove insoluble debris. The supernatants were transferred to HPLC vials with inserts and stored at –20 °C before LC–MS analysis. The Folch method was used to extract the lipids from OPCs treated with T3 and DMSO for 6 d. A mixture of 600 μL chloroform/MeOH (2:1; v/v) was used in the freeze-thaw extraction method as described above, and a subsequent addition of 600 μL of water was performed. Using this liquid–liquid extraction method, the organic phase was collected, dried and finally reconstituted in IPA/MeOH/H₂O (5:1:4; v/v/v) before analysis.

Cell extracts were analyzed on a 6550 iFunnel QTOF mass spectrometer (Agilent Technologies) coupled with a 1290 UPLC system (Agilent Technologies). For global metabolomics, HPLC was carried out on a Luna Aminopropyl, 3 μm , 150 mm \times 1.0 mm I.D. HILIC column (Phenomenex). The mobile phase was composed of A = 20 mM ammonium acetate and 40 mM ammonium hydroxide in 95% water (v/v) and B = 95% acetonitrile; the remaining 5% components were either acetonitrile or water, respectively. A linear gradient from 100% B (0–5 min) to 100% A (50–55 min) was applied. A 10-min re-equilibration time was applied to the HILIC column for re-equilibration and maintenance of reproducibility. The flow rate was 50 $\mu\text{L}/\text{min}$, and the sample injection volume was 5 μL . ESI source conditions were set as follows: dry gas temperature, 200 °C; flow, 11 L/min; fragmentor, 380 V; sheath gas temperature, 300 °C; flow, 9 L/min; nozzle voltage, 500 V; capillary voltage, –500 V in ESI negative mode. The instrument was set to acquire data over the m/z range of 50–1,000, with the MS acquisition rate of 1 spectra/s. The sample sequence was randomized to avoid systematic decreases in signals over sample sets. For the MS/MS of selected precursors, the default isolation width was set as narrow ($\sim 1.3 m/z$), with a MS acquisition rate at 2 spectra/s and MS/MS acquisition at 2 spectra/s to acquire over the m/z range 50–1,000 and 25–1,000, respectively. MS/MS data were acquired at the collision energy of 20 V and 40 V.

For the lipidomics profiling, the separation was conducted using an Agilent ZORBAX Eclipse Plus RRHD C18 column (2.1 \times 100 mm, 1.8 μm).

The mobile phase contains A (5:1:4 IPA/MeOH/H₂O with 5 mM NH₄OAc and 0.1% CH₃COOH) and B (99:1 IPA/H₂O with 5 mM NH₄OAc and 0.1% CH₃COOH). The mobile phase starts with 0% B for 3 min and increases to 20% B in the following two minutes. The gradient gradually increases to 30% B until 25 min and further to 95% B in next 10 min, which is maintained for 2 min. Subsequently, the mobile phase is set to the original 0% B (37–38 min) and another 10 min re-equilibration time was applied to for re-equilibration. The flow rate is 0.35 mL/min and the temperature keeps at 50 °C.

LC–MS data were converted to mzXML files using Masshunter Acquisition Software (Agilent Masshunter 6.0B). The mzXML files were uploaded to XCMS Online web platform for data processing (<https://xcmsonline.scripps.edu>)⁴⁵ including peak detection, retention time correction, profile alignment, and isotope annotation. Data were processed using both pair-wise and multigroup comparison, and the parameter settings were as follows: centWave for feature detection ($\Delta m/z = 15$ p.p.m.; minimum peak width = 10 s; and maximum peak width = 60 s); obiwarp settings for retention time correction (profStep = 0.5); and parameters for chromatogram alignment, including mzwid = 0.015, minfrac = 0.5, and bw = 5. The relative quantification of metabolite features was based on extracted ion chromatogram (EIC) areas. Paired parametric t-test and one-way ANOVA (post-hoc Tukey test) were used to test the variation pattern of metabolite features between and across cell samples collected at different times after being treated with T3 and DMSO. Multiple group analysis and pairwise comparisons between DMSO and T3 at individual incubation time were conducted. The results output, including EICs, pairwise/multigroup cloud plot, multidimensional scaling plots, and principle components were exported directly from XCMS Online. Generally, the numbers of total pairwise comparison features and significantly altered features (statistically defined as $P < 0.01$, including both upregulated and downregulated features) were reported in this study.

Targeted multiple pathway analysis. The metabolites in the upstream and downstream of taurine and creatine pathways are of great interest in this study. Due to the poor stability of several sulfur-containing compounds including cysteine, GSH and GSSG, a different extraction method from the global metabolomics was developed and validated. Briefly, cell pellets were extracted with 150 μL 75% ACN in water modified with 0.1% formic acid using the freeze-thaw method mentioned above. Samples were centrifuged at 16,000g and 4 °C for 15 min, and the supernatant was directly injected into the Agilent triple-quad (QQQ, Agilent 6495). It was operated in multiple reaction monitoring mode (MRM), in which the collision energies and product ions (MS2 or quantifier and qualifier ion transitions) were pre-optimized for each metabolite of interest (**Supplementary Table 1**). Cycle time was 50 ms for each transition. ESI source conditions were set as the following: gas temperature, 250 °C; gas flow, 14 L/min; nebulizer, 20 psi; sheath gas, 250 °C; sheath gas flow, 11 L/min; capillary voltage, 3,000 V; nozzle voltage, 1,500 V; and EMV, 1,000 V in ESI positive mode. The analyses were performed on the Imtakt Amino Acid column (length 150 \times i.d. 2 mm, particle size 3 μm). The mobile phase was composed of A = 50 mM ammonium formate in water (v/v) and B = 100% acetonitrile in 0.1% formic acid. A linear gradient from 70% B (0–1 min) to 70% A (1–12 min, maintaining for 2 min) was applied. A 12-min re-equilibration time was applied to the column for re-equilibration. The flow rate was 200 $\mu\text{L}/\text{min}$, and the sample injection volume was 20 μL .

High-content imaging. For dose–response co-treatment experiments, black, clear-bottom 384-well plates (Greiner) were coated with poly-D-lysine (10 $\mu\text{g}/\text{mL}$ in PBS). Miconazole and benzotropine were added at 8 doses in differentiation media; three-fold dilutions down from 10 μM . Taurine was then added at 8 concentrations; three-fold dilutions down from 20 mM. This 384-well format was also used for experiments combining benzotropine (0.5 μM), miconazole (2 μM) or T3 (1 μM) with propargylglycine (0.1, 3, 10 or 30 μM), reduced glutathione (1, 10, 30 or 100 μM) or ascorbic acid (1, 10, 30 or 100 mM). OPCs were then seeded at a density of 1,000 cells per well, and the plates were incubated at 37 °C with 5% CO₂ for 6 d. For time-course experiments, cells were seeded at a density of 5,000 cells per well in poly-D-lysine-coated 96-well plates. Cells were treated with DMSO (0.1%), benzotropine (0.5 μM), miconazole (2 μM) or T3 (1 μM) on day 0, and taurine (20 mM) was added

at 0, 1 or 3 d post-drug treatment. The plates were incubated at 37 °C with 5% CO₂ for 6 d. On day 6, cells were then fixed for 20 min with 4% formaldehyde solution and stained with anti-MBP antibody (cat. #MAB382, Millipore) or anti-A2B5 antibody (cat. #MAB312, Millipore) in 3% BSA, 0.3% Triton X-100 with overnight incubation at 4 °C. The cells were washed and incubated with secondary antibody (Alexa Fluor 488 goat anti-mouse IgG, Life Technologies) and DAPI (Invitrogen) for 1 h at room temperature. The cells were washed and plates were sealed and imaged using an Opera confocal imaging reader (PerkinElmer) or a Cellomics Cell Insight imaging reader (Thermo). An air ×10 lens was used to capture nine images per well at both wavelengths (488 and 365 nm), with each image representing a different unique locations field in a single well. For image analysis, DAPI-stained nuclei and MBP-positive or A2B5-positive cell bodies were detected using an algorithm that selects for positive cell bodies and nuclei within a range of fluorescent emission values and sizes as determined by fitting parameters to positive (T3, 1 μM) and negative (DMSO, 0.1%) controls. The number of DAPI-positive objects were enumerated in experiments where cell counts were required. Numerical results from the analyzed images were later exported for analysis using Excel (Microsoft) and/or Genedata software.

Cell viability analysis. In poly-D-lysine-coated white 384-well plates (Greiner), benztropine (0.5 μM), miconazole (2 μM) or T3 (1 μM) were added in combination with rotenone (0.1, 1, 3 or 10 μM) or oligomycin (0.1, 1, 3 or 10 μM). Cells were then seeded at a density of 1,000 cells per well, and the plates were incubated at 37 °C with 5% CO₂ for 1, 3 or 6 d. At these three time points, the CellTiter-Glo Luminescent Cell Viability Assay (Promega) was used to analyze cytotoxicity.

Detection of caspase 3/7. In poly-D-lysine-coated white 96-well plates (Greiner), cells were seeded at 5,000 cells per well. Taurine (20 mM) was added on days 0 or 3, alone and in combination with benztropine (0.5 μM), miconazole (2 μM), T3 (1 μM) or staurosporine (1 μM) added on day 0. The Caspase-Glo 3/7 Assay (Promega) was used to quantify caspase-3/7 activity 6, 24 and 48 h after drug and taurine addition on day 0. Caspase-3/7 activity was also measured 24, 48 and 72 h (days 4, 5 and 6) after taurine addition on day 3.

In vitro OL maturation assay. Cortical and hippocampal tissue was dissected from C57BL/6 mice at embryonic day 14 and dissociated in 0.5% trypsin with 100 U/mL DNase I diluted in HBSS (+/+) for 10 min at 37 °C. The reaction was stopped by supplementing to a final concentration of 10% v/v FBS, 100 μg/mL Soybean Trypsin Inhibitor and 10 U/mL DNase I. Cells were resuspended in plating media consisting of equal volumes of FCS, HBSS (+/+), high-glucose DMEM with L-glutamine, and F-12 with L-glutamine, and then plated onto acid prewashed German glass coverslips coated with 50 μg/mL poly-D-lysine and 20 μg/mL laminin at a density of 50,000 cells/cm². Cells were allowed to attach for 2 h and then coverslips were rinsed with PBS before being transferred to a 24-well plate containing 0.5 mL growth media consisting of: Neurobasal medium, B27 supplement (Gibco), 0.5× Glutamax (Thermo), 5 μg/mL gentamycin and 5 μM glutamic acid. Half of the cell media was replaced after 3 days in culture with supplemental growth media not containing glutamic acid⁴⁶. After 5 days in culture, rat-derived cortical OPCs were added to the neuronal culture at a density of 5,000 cells/cm². Co-culture media was used to resuspend and plate OPCs consisting of a 1:3 mixture of neuronal growth supplement (as above) and oligodendrocyte differentiation media, containing DMEM/F-12 (with L-glutamine), insulin-free N2 supplement, 1× Glutamax, 1× MEM nonessential amino acids, 1× β-mercaptoethanol, 2 ng/mL PDGF and 5 μg/mL gentamycin. All drugs and taurine co-treatment were added once to the culture upon plating of OPCs at the following concentrations: 0.5 μM benztropine and 1.0 μM miconazole, each with or without 2 mM taurine. Cultures were maintained by replacing half of the media every 3 d, maintaining an equivalent concentration of taurine throughout in appropriate wells. Fourteen days after addition of OPC and drug treatments co-cultures were fixed for 15 min in 4% PFA and stained sequentially overnight with TUJ1 (cat. #MMS-435P, Covance) and MBP (cat. #ab134018, Abcam) antibodies, each immediately followed by associated secondary antibodies (Alexa Fluor 488 goat anti-mouse IgG, Life Technologies; Cy3 goat anti-chicken, Jackson ImmunoResearch) (Thermo)

and Cy3-Goat anti-Chicken (Jackson ImmunoResearch) and 1 μg/mL DAPI for nuclear counterstain. Immunostained coverslips were then S7 invert mounted on glass slides using Fluoromount G (Southern Biotech). Randomly selected regions of 25 fields or greater were imaged at 63× magnification using a Zeiss 780 confocal microscope. Z-projection images were then rendered in Imaris (Bitplane) to identify apposition of oligodendrocyte and neuronal processes. Colocalization was quantified within regions of interest delineated at the periphery of individual oligodendrocytes. The colocalization index (adapted from a previously described method⁴⁷) was calculated as the total proportion of colocalized 3D surface area between Tuj1 (neuron) and oligodendrocyte (MBP) over total Tuj1 (neuronal process) area enclosed within each oligodendrocyte process tree as the selected region of interest (ROI; see Fig. 3b). Mean colocalization values for each condition were normalized to the DMSO condition mean analyzed statistically using Prism software (GraphPad, v7) for two-way ANOVA comparisons (drug treatment × taurine supplement) with Tukey's post-tests for statistical significance.

Statistical comparison of myelination in drug-treated co-cultures as well as drug-treated co-cultures with taurine supplement showed a significant main effect for benztropine ($F(1,56) = 27.82$; $P < 0.0001$) and taurine supplement ($F(1,56) = 10.8$; $P = 0.0018$), with significant Tukey post-hoc results for benztropine alone vs. DMSO ($q = 3.19$; $P = 0.0442$), benztropine + taurine vs. DMSO ($q = 8.48$; $P < 0.0001$) and benztropine + taurine vs. benztropine alone ($q = 5.09$; $P = 0.0037$). Additionally, there was a significant main effect for miconazole treatment ($F(1,46) = 24.9$; $P < 0.0001$) and a main effect for taurine ($F(1,46) = 10.55$; $P < 0.0022$). Tukey's post-hoc tests showed no significant difference for miconazole alone vs. DMSO ($q = 3.61$; $P = 0.065$); however, there was a significant difference for miconazole + taurine vs. DMSO ($q = 8.24$; $P < 0.0001$) and miconazole + taurine vs. miconazole alone ($q = 4.54$; $P = 0.0125$). Taurine treatment alone showed no significant difference vs. DMSO in either benztropine and miconazole experiments ($P = 0.58$ and $P = 0.54$, respectively).

Western blot analysis. OPCs were plated in basal differentiation medium at 1.7×10^5 cells/well and treated for 6 d with benztropine (0.5 μM), miconazole (2 μM) with and without the tested endogenous metabolites, T3 (1 μM) or DMSO. After washing with PBS, cells were collected in ice-cold RIPA buffer containing protease and phosphatase inhibitors. Following incubation on ice for >20 min and sonication, lysed cells were centrifuged (16,000g for 15 min at 4 °C). Total protein was quantified using a BCA analysis, and 25 μg of protein from each sample was denatured by boiling with Bolt LDS Sample Buffer (4×) and Sample Reducing Agent (10×). Proteins were electrophoresed using Bolt 4–12% Bis-Tris gels (Life Technologies) and transferred to a PVDF membrane (Bio-Rad). The membrane was blocked with Odyssey PBS Blocking Buffer (LI-COR) and incubated overnight at 4 °C with anti-MBP antibody (cat. #MAB382, Millipore) and anti-actin anti-β-actin antibody (cat. #sc-47778). Blots were incubated with HRP-conjugated secondary donkey anti-mouse antibody (IRDye800CW, LI-COR) and imaged using Odyssey CLx and Image Studio (LI-COR).

Mitochondrial respiration assay. Cellular oxygen consumption rate (OCR) was measured using an XFe96 extracellular flux analyzer (Seahorse Biosciences). OPCs were seeded at 40,000 cells/well in poly-D-lysine-coated XFe96 plates and cultured for 6 d with taurine (2 and 20 mM) alone, or together with miconazole and benztropine. Cells were then incubated in assay medium (DMEM with 20 mM glucose, 5 mM pyruvate and 5 mM sodium bicarbonate, pH ~ 7.4) for at least 30 min before the assay. Media to deliver a final well concentration corresponding to 1 μM oligomycin, 2 μM carbonyl cyanide 4-(trifluoromethoxy) phenylhydrazone (FCCP) and 2 μM rotenone + 2 μM antimycin A were preloaded into the compound delivery ports of the system. The assay starts with the recording of the basal OCR, which is followed by recording of the OCR in response to different compounds that constitute the Mitochondria Stress Test (Seahorse Biosciences, Agilent). Once the basal OCR was measured, the compounds were added sequentially and the effects on OCR measured 3 times every 5 min. Oligomycin blocks ATP synthase; FCCP dissipates the inner membrane potential enabling maximum electron flux through the electron transport chain (ETC); rotenone + antimycin A inhibit complexes I and III,

respectively, thereby blocking the entry of electrons in the ETC and shutting down mitochondrial activity.

Statistical analysis. Unless otherwise stated, data represent mean \pm s.d. of representative experiments. Unless otherwise stated, statistical analysis was performed using Prism software (GraphPad, v7) for one-way ANOVA comparisons with Tukey's post-tests for statistical significance.

Life sciences reporting summary. Further information on experimental design and reagents is available in the **Life Sciences Reporting Summary**.

Data availability. The data that support the findings of this study are available from the corresponding author upon reasonable request.

45. Tautenhahn, R. *et al.* XCMS online: A web-based platform to process untargeted metabolomic data. *Anal. Chem.* **84**, 5035–5039 (2012).
46. Pang, Y. *et al.* Neuron-oligodendrocyte myelination co-culture derived from embryonic rat spinal cord and cerebral cortex. *Brain Behav.* **2**, 53–67 (2012).
47. Diemel, L.T., Wolswijk, G., Jackson, S.J. & Cuzner, M.L. Remyelination of cytokine- or antibody-demyelinated CNS aggregate cultures is inhibited by macrophage supplementation. *Glia* **45**, 278–286 (2004).

Life Sciences Reporting Summary

Nature Research wishes to improve the reproducibility of the work that we publish. This form is intended for publication with all accepted life science papers and provides structure for consistency and transparency in reporting. Every life science submission will use this form; some list items might not apply to an individual manuscript, but all fields must be completed for clarity.

For further information on the points included in this form, see [Reporting Life Sciences Research](#). For further information on Nature Research policies, including our [data availability policy](#), see [Authors & Referees](#) and the [Editorial Policy Checklist](#).

▶ Experimental design

1. Sample size

Describe how sample size was determined.

For metabolomics studies, we performed preliminary experiments with $n=3$ to determine the variability between biological replicates in each treated group. Based on the power analysis, we made the determination to use $n=5$ for the cells treated under each condition. For Western blot-based analysis experiments with $n=3$ were performed to achieve robust significance between vehicle and drug (e.g., benztropine or miconazole). For high content imaging-based assays sample sizes of greater than or equal to 3 were used to achieve robust significance between vehicle and drug (e.g., benztropine or miconazole). For confocal microscopy-based colocalization assays, power analysis was used to determine that $n > 8$ was required to achieve significance between vehicle and drug (i.e., benztropine).

2. Data exclusions

Describe any data exclusions.

We did not exclude any samples from the data analysis.

3. Replication

Describe whether the experimental findings were reliably reproduced.

Experimental findings were reliably reproduced >2 times, unless otherwise stated.

4. Randomization

Describe how samples/organisms/participants were allocated into experimental groups.

For metabolomics experiments, we randomized the sample injection order in the experiments to minimize the affect of instrument signal drift.

5. Blinding

Describe whether the investigators were blinded to group allocation during data collection and/or analysis.

In order to perform the metabolomic pair-wise comparisons it is required to input the group allocation. In other experiments blinding is not applicable, as automated analysis was performed.

Note: all studies involving animals and/or human research participants must disclose whether blinding and randomization were used.

6. Statistical parameters

For all figures and tables that use statistical methods, confirm that the following items are present in relevant figure legends (or in the Methods section if additional space is needed).

- n/a Confirmed
- The exact sample size (n) for each experimental group/condition, given as a discrete number and unit of measurement (animals, litters, cultures, etc.)
 - A description of how samples were collected, noting whether measurements were taken from distinct samples or whether the same sample was measured repeatedly
 - A statement indicating how many times each experiment was replicated
 - The statistical test(s) used and whether they are one- or two-sided (note: only common tests should be described solely by name; more complex techniques should be described in the Methods section)
 - A description of any assumptions or corrections, such as an adjustment for multiple comparisons
 - The test results (e.g. P values) given as exact values whenever possible and with confidence intervals noted
 - A clear description of statistics including central tendency (e.g. median, mean) and variation (e.g. standard deviation, interquartile range)
 - Clearly defined error bars

See the web collection on [statistics for biologists](#) for further resources and guidance.

► Software

Policy information about [availability of computer code](#)

7. Software

Describe the software used to analyze the data in this study.

Masshunter Acquisition Software (Agilent), XCMS Online web platform (TSRI), Genedata Screener (Genedata), Image Studio (LI-COR Biosciences), Seahorse XF (Seahorse Biosciences), Metaboanalyst (<http://www.metaboanalyst.ca/>), Prism (GraphPad, v7)

For manuscripts utilizing custom algorithms or software that are central to the paper but not yet described in the published literature, software must be made available to editors and reviewers upon request. We strongly encourage code deposition in a community repository (e.g. GitHub). *Nature Methods* [guidance for providing algorithms and software for publication](#) provides further information on this topic.

► Materials and reagents

Policy information about [availability of materials](#)

8. Materials availability

Indicate whether there are restrictions on availability of unique materials or if these materials are only available for distribution by a for-profit company.

Materials are available from commercial sources. OPCs and primary mouse neurons were isolated in-house.

9. Antibodies

Describe the antibodies used and how they were validated for use in the system under study (i.e. assay and species).

Anti-Myelin Basic Protein antibody: EMD Millipore, MAB382, a.a. 129-138, clone 1.
 Anti-A2B5 antibody: EMD Millipore, MAB312, clone A2B5-105.
 Secondary antibody for western blot analysis: HRP-conjugated donkey anti-mouse antibody; IRDye 800CW Donkey anti-Mouse IgG H&L (LI-COR).
 Secondary antibody for high content imaging analysis: Goat Anti-Mouse IgG H&L (Alexa Fluor 488; Invitrogen).
 Antibodies used in OPC/Neuronal co-culture assay: Anti-Myelin Basic Protein antibody (chicken; AbCam), TUJI (rabbit; Covance), Cy3-Goat anti-Chicken (JacksonImmuno Research).

10. Eukaryotic cell lines

a. State the source of each eukaryotic cell line used.

OPCs: Primary rat optic nerve-derived
 Neurons: Primary mouse primary cortical tissue-derived

b. Describe the method of cell line authentication used.

NA; Primary cell lines

c. Report whether the cell lines were tested for mycoplasma contamination.

Yes

d. If any of the cell lines used are listed in the database of commonly misidentified cell lines maintained by [ICLAC](#), provide a scientific rationale for their use.

NA

▶ Animals and human research participants

Policy information about [studies involving animals](#); when reporting animal research, follow the [ARRIVE guidelines](#)

11. Description of research animals

Provide details on animals and/or animal-derived materials used in the study.

Primary mouse neurons were isolated from cortical and hippocampal tissues from C57BL/6 mice at embryonic day 14. OPCs were purified from postnatal day 6 rat optic nerve to greater than 99% purity by sequential immunopanning.

Policy information about [studies involving human research participants](#)

12. Description of human research participants

Describe the covariate-relevant population characteristics of the human research participants.

NA